Advanced Statistical Techniques for Noninvasive Hyperglycemic States Detection in Mice Using Millimeter-Wave Spectroscopy

Aldo Moreno-Oyervides, M. Carmen Aguilera-Morillo, Fernando Larcher, Viktor Krozer, *Senior Member, IEEE*, and Pablo Acedo

***Abstract*—In this article, we discuss the use of advanced statistical techniques (functional data analysis) in millimeter-wave (mm-wave) spectroscopy for biomedical applications. We employ a W-band transmit–receive unit with a reference channel to acquire spectral data. The choice of the W-band is based on a tradeoff between penetration through the skin providing an upper bound for the frequencies and spectral content across the band. The data obtained are processed using functional principal component logit regression (FPCLoR), which enables to obtain a predictive model for sustained hyperglycemia, typically associated with diabetes. The predictions are based on the transmission data from noninvasive mm-wave spectrometer at W-band. We show that there exists a frequency range most suitable for identification, classification, and prediction of sustained hyperglycemia when evaluating the functional parameter of the functional logit model (β). This allows for the optimization of the spectroscopic instrument in the aim to obtain a compact and potential low-cost noninvasive instrument for hyperglycemia assessment. Furthermore, we also demonstrate that the statistical tools alleviate the problem of calibration, which is a serious obstacle in similar measurements at terahertz and IR frequencies.**

***Index Terms*—Functional data analysis (FDA), functional principal components logit regression (FPCLoR), millimeter-wave (mm-wave) spectroscopy, noninvasive diagnostics, sustained hyperglycemia, W-band reflectometer, W-band transmit/receive unit.**

Manuscript received May 29, 2019; revised September 11, 2019 and October 27, 2019; accepted January 7, 2020. Date of publication January 16, 2020; date of current version May 1, 2020. This work was supported in part by the Spanish Ministry of Economy and Competitiveness under Project TEC2017-86271-R, in part by the Instituto de Salud Carlos III (Spain) under Grant DTS17/00135, in part by the Ministerio de Economía y Competitividad, FEDER funds under Project MTM2017-88708-P, and in part by the Agencia Estatal de Investigación, Ministerio de Ciencia, Innovación y Universidades under Project IJCI-2017-34038. The work of Aldo Moreno-Oyervides was supported by the Consejo Nacional de Ciencia y Tecnología de México (CONACYT). *(Corresponding author: Aldo Moreno-Oyervides.)*

Aldo Moreno-Oyervides and Pablo Acedo are with the Department of Electronics Technology, Universidad Carlos III de Madrid, 28911 Madrid, Spain, and also with the Instituto de Investigaciones Sanitarias de la Fundación Jiménez Díaz, 28015 Madrid, Spain (e-mail: aldmoren@ing.uc3m.es; pag@ing.uc3m.es).

M. Carmen Aguilera-Morillo is with the Department of Applied Statistics and Operational Research, and Quality, Universitat Politécnica de València, 46022 Valencia, Spain, and also with Santander Big Data Institute, Universidad Carlos III de Madrid, Getafe, Madrid 28903, Spain (e-mail: maguiler@est-econ.uc3m.es).

Fernando Larcher is with the Department of Bioengineering, Universidad Carlos III de Madrid, 28911 Madrid, Spain, and also with the Instituto de Investigaciones Sanitarias de la Fundación Jiménez Díaz, 28015 Madrid, Spain, with the Epithelial Biomedicine Division, Centro de Investigaciones Energéticas Medioambientales y Tecnológicas, 28040 Madrid, Spain, and also with the Centro de Investigación Biomédica en Red de Enfermedades Raras, 28029 Madrid, Spain (e-mail: fernando.larcher@ciemat.es).

Viktor Krozer is with the Universidad Carlos III de Madrid, 28903 Getafe, Spain, on leave from the Physics Institute, Goethe University Frankfurt am Main, Frankfurt am Main 60438, Germany (e-mail: krozer@physik.uni-frankfurt.de).

Color versions of one or more of the figures in this article are available online at https://ieeexplore.ieee.org.

Digital Object Identifier 10.1109/TTHZ.2020.2967236

I. Introduction

MILLIMETER-WAVE (mm-wave) spectroscopy has received much attention for biomedical applications, due to its spectral resolution, high sensitivity, measurement speed, and richness in the information contained in the acquired spectrum. Many biomedical applications have been addressed recently utilizing mm-wave spectroscopy [1]–[5], being diabetes detection one of the first applications envisaged for this technique. Microwave, mm-wave, and terahertz spectroscopy have been proposed for diabetes mellitus (DM) diagnostic associated with instantaneous glucose level measurement [6]–[10] and sustained hyperglycemia states detection [11], both relevant to the diagnostic and patient control. However, in both cases, we are still far from an operational diagnostic based on these techniques that leverage the advantages identified for such a system, such as noninvasiveness, the use of nonionizing radiation, and the potential low cost of the developed system.

DM is a very complicated metabolic disorder affecting a great part of the world population, which is severely increased every year [12]–[16]. This metabolic disorder, which is characterized by the presence of high-blood glucose content known as "Hyperglycemia" [17], brings several and serious irreversible health consequences if it is not detected and treated on time, such as heart attacks, strokes, kidney failure, and vision loss [18], [19]. The current medical procedures for diabetes control are mainly based on invasive technologies facing multiple disadvantages: high follow-up costs, painful in some cases, and disturbing in daily life, which explains somehow the unwillingness of people to completely follow medical recommendations in diabetes care. Therefore, there is a worldwide effort to develop new technologies that are able to diagnose and monitor diabetes noninvasively (or minimally invasive), improving the existing medical procedures, especially using spectroscopic techniques but with limited success due to the lack of accuracy or feasibility of the

proposed spectroscopic technique [20]–[24]. Furthermore, the measure of free glucose in the blood as the diagnostic parameter for diabetes also has its drawbacks, as blood glucose level is strongly conditioned by many physiological processes, such as eating, exercise, or the related ones to strong emotions. Hence, new noninvasive techniques that reduce the influence of external factors, thus enhancing the diagnosis and monitoring of diabetes, are needed.

An important indicator of DM is hyperglycemia, generally caused by DM and having a strong impact on the physiological functions of the organism. The formation of advanced glycation end-products associated with the sustained high-glucose concentration in blood is responsible for the most relevant complications associated with DM. An early and noninvasive diagnostic for such sustained hyperglycemic states is crucial, not only for diabetes diagnostics thus facilitating an early intervention to regulate the carbohydrate metabolism but also for the metabolomic control and supervision of the patients.

This article proposes an mm-wave reflect/transmit setup using a multiplied source and subharmonic Schottky diode receivers and appropriate statistical spectroscopy techniques to arrive at a diagnostic tool for noninvasive control of sustained hyperglycemic state. The focus of the article is on the discussion of the importance of using adequate statistical techniques to process the spectral data in mm-wave spectroscopy to develop biomedically relevant diagnostic systems as, for example, in DM diagnostic.

Until now, multivariate statistical techniques have been widely used for data analysis and statistical modeling in spectroscopic applications (e.g., [25]–[29]), and for the optimization of the frequency spectrum used for interrogation (e.g., [30] and [31]). In biomedical spectroscopic applications, the acquired data correspond to complicated spectra with overlapping responses from many different constituents of the biomedical sample. This overlap of spectral responses prevents the isolation of a specific component within the sample and perform spectral classification. In addition, other factors adversely affecting the spectral classification, such as environmental influences, instrument noise, and interferences by physiological processes, have an impact on the spectral data and necessitate the systematic analysis of a set of discrete and independent variables. The acquired spectral data might become very large and lead to dimensionality problems, hindering data processing, and requiring dedicated statistical analysis. The functional data analysis (FDA) [32] is currently employed in biomedical applications based on spectroscopic techniques [33], [34] since it provides a set of more suitable and powerful statistical tools for the processing and analysis of the spectral information.

We demonstrate in this article a spectrometer working in the W-band (75–110 GHz) with reflect and transmit measurement capabilities using a nonspecific approach. In this way, the proposed technique allows us to discriminate the metabolic animal condition (normoglycemic or hyperglycemic) without the need to isolate or quantify the specific response of a single component or metabolite. To achieve this, we employ the FDA to obtain a continuous representation (function) from each spectrum measured at discrete frequencies within the W-band.

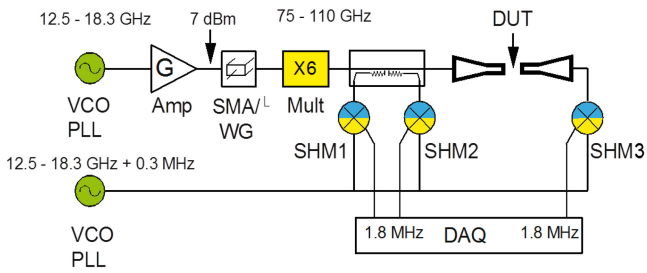

Fig. 1. Simplified block diagram of the setup. See text for details.

Continuous representation of the spectrum using the FDA allows for better flexibility for high-dimensional data and longitudinal data analysis, as well as improves spectral variability analysis.

In our spectral analysis, we apply the functional principal component logit regression (FPCLoR) [35] to obtain a predictive model as a diagnostic tool for hyperglycemia in the animal models. We study qualitatively and quantitatively how the obtained spectral response characterizes the hyperglycemia condition in the animal models by interpreting the FPCLoR model. Finally, we demonstrate that the frequency bandwidth can be halved using the FPCLoR model when choosing the main contributing frequencies to hyperglycemia discrimination. These results show the potential of the FDA establishing a feedback to the W-band spectral results and the spectroscopic analysis tool presented here.

The article is organized as follows. In Section II, we describe the spectroscopic instrument and methods of sample preparation. In Section III, we study and discuss the data acquisition and the data processing algorithms, and in Section IV, we discuss the achieved results. Finally, the article concludes in Section V.

II. Materials and Methods

A. MM-Wave Spectroscopy Instrument

The spectral interrogation for the noninvasive assessment of sustained hyperglycemia was carried out by a spectrometer operating across the full W-band with steps of 1.5 GHz. As shown in Fig. 1, generators deliver a swept signal in the Ku-band (12.5–18.5 GHz in steps of 0.25 GHz) with 0.3 MHz frequency difference between the two signals. One signal generator is connected to an active frequency sixtupler (MULT), resulting in a frequency sweep within the W-band. The MULT is realized in a waveguide housing and exhibits a WR10 waveguide output. The output signal from the MULT is fed to a dual-directional coupler. The coupled arms of the coupler define the reference and reflect channels, respectively, with subharmonic mixer receivers at each coupled port. The branch of the coupler is fed into a waveguide probe and device under test. The transmission path is measured with equivalent subharmonic mixer receivers, as in the reference and reflect ports. The outputs of the subharmonic receivers deliver an intermediate frequency of IF = 1.8 MHz and are connected to a data acquisition unit (Handyscope HS4-10, TiePie engineering, Sneek, Netherlands), which digitizes the measured signals with a sampling rate of 10 MHz. Finally, all the sampled signals are filtered and processed using LabVIEW software.

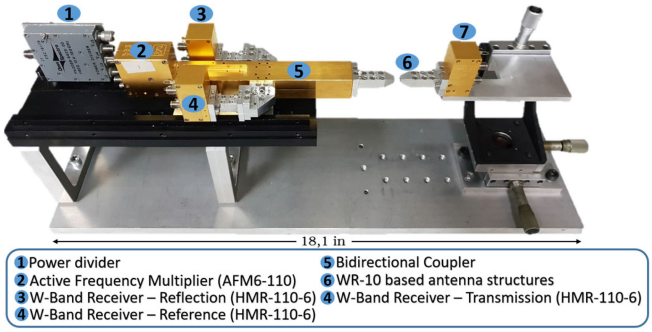

Fig. 2. MM-wave spectroscopic instrument for the noninvasive sustained hyperglycemia assessment.

More details of the spectrometer already reported can be found in [11] and [36]. Fig. 2 shows a photograph of the mm-wave instrument identifying all the components mentioned above.

In the present article, we exclusively employ transmission amplitude measurements, even though phase results are also available, as the amplitude values are sufficient for the FPCLoR analysis. The output power of the signal generator was adjusted to obtain a flat frequency response at the transmission port without the biological sample. No previous calibration is required for the amplitude data. These aspects enormously simplified the diagnostic system and allow for further low-cost and compact implementations.

B. Experimental Protocol

The mm-wave spectroscopic measurements were performed at the Centro de Investigaciones Energéticas, Medioambientales, y Tecnológicas (CIEMAT) Laboratory Animals Facility (Spanish registration number 28079-21 A), which provided the animal models. The animals were not subjected to special treatments before the mm-wave measurements. Mice hair were regularly cut to ensure and facilitate the positioning of the probes but were not totally shaved. The insensitivity of the measured results to hair skin in mice was proven earlier in [7]. Prior to the measurement process, each mouse was anesthetized to prevent movement and self-harm risks during the measurements. Two anesthesia methods were followed to carefully avoid the impact of anesthesia treatment. In experiment A, the anesthesia was administered by injection using standard rodent anesthesia (ketamine/medetomidine). Then, for experiment B, the mice were anesthetized by inhalation using isoflurane mixed with oxygen, which reduces the induction time and is less harmful to animals.

As shown in Fig. 3, mice were assessed one by one and the spectral interrogation was performed directly on a fold of the skin on the back of each mouse. The probes of the spectrometer instrument were two previously aligned straight cuts of a WR10 waveguide tapered on the outside to facilitate the skinfold. The separation between the straight cuts was fixed to hold the skinfold without harming the animal. The measuring process takes around 45 sec and the anesthetic gas was continuously supplied to the animal via a mask during the whole period in experiment B. The measurement time is mainly limited by the control electronics and not by the mm-wave instrument.

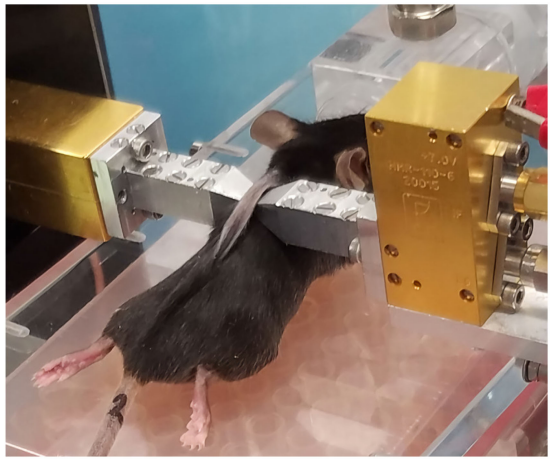

Fig. 3. Photograph taken during the measuring process.

TABLE I
SAMPLES POPULATION DESCRIPTION

Experiment	Condition	Type	Mean glucose level	Label	Quantity
A	Normoglycemia	-	136 mg/dl	Healthy	10
	Hyperglycemia	Leptin-deficient	180 mg/dl	Obese	5
	Hyperglycemia	Insulin-resistant	500 mg/dl	Diabetic	5
B	Normoglycemia	-	144 mg/dl	Healthy	18
	Hyperglycemia	Leptin-deficient	245 mg/dl	Obese	9
	Hyperglycemia	Insulin-resistant	380 mg/dl	Diabetic	6

All experimental procedures were carried out according to European and Spanish laws and regulations (European convention ETS 1 2 3, about the use and protection of vertebrate mammals used in experimentation and other scientific purposes, Directive 2010/63/UE and Spanish Law 6/2013, and R.D. 53/2013 about the protection and use of animals in scientific research). Procedures were approved by the Animal Experimentation Ethical Committee of the CIEMAT according to all external and internal biosafety and bioethics guidelines, and by Spanish competent authority with registered number PROEX 176/15.

C. Sample Population

Two experiments were conducted with 16 months elapsed between the first and second experiment, and a different sample of mice for each experiment referred to as "A" and "B." In both experiments, the sample of mice included animals with normoglycemic and hyperglycemic conditions. Healthy mice of different strains with an expected blood glucose level of 100 mg/dL were considered as normoglycemic animals. Within the hyperglycemic cases, two different types of hyperglycemia were considered: obese mice due to a genetic mutation that causes a deficiency of leptin (Lep^{ob}/ Lep^{ob}) and diabetic mice due to a genetic mutation that causes insulin resistance (Lep^{db}/ Lep^{db}) [37]. The expected glucose level for the hyperglycemic cases is above 150 mg/dL and 250 mg/dL for the obese mice and the diabetic mice, respectively. Table I summarizes the sample of mice measured at each experiment.

All animals were purchased from Elevage–Janvier (France) and housed individually in pathogen-free conditions at CIEMAT.

III. Data Processing and Statistical Analysis

As described in Section II, the spectroscopic measurement provides a one-dimensional array (vector) whose entries correspond to a finite set of observed amplitudes for each frequency. This vector is then transformed into a continuous function of frequency, which allows the application of the FDA [32].

A. Functional Data Approximation

Measurements are usually affected by systematic errors, noise, and/or other external interferences. Therefore, data are assumed to be smooth but observed with an associated error, in our case

$$x_{ik} = x_i(f_{ik}) + \epsilon_{ik}, \quad k = 1, \ldots, m, \quad i = 1, \ldots, n \tag{1}$$

where x_{ik} is the *i*th discrete sample path (raw spectra), $x_i(f_{ik})$ is a smooth function observed at the frequency points f_{ik}, and ϵ_{ik} is an error term representing noise, with *n* being the sample size (number of assessed mice) and *m* being the number of frequency points. Then, the function is approximated by assuming that the sample paths belong to a finite-dimensional space generated by an orthogonal basis $\{\phi_1(f), \ldots, \phi_p(f)\}$, so that

$$x_i(f) = \sum_{j=1}^{p} a_{ij}\phi_j(f), \quad f \in F, \quad i = 1, \ldots, n \tag{2}$$

where $x_i(f)$ is the estimated curve, a_{ij} are the basis coefficients, $\phi_j(f)$ are the basis functions, and *F* is the observation interval (frequency interval). Since our data are smooth but observed with some noise, a basis of smooth functions must be considered. Cubic B-splines basis generates the space of splines of degree three, defined as curves consisting of piecewise polynomial of degree three that join up smoothly in a set of nodes with continuity in their derivatives up to order two [38]. Regression splines and P-splines can be used to estimate the basis coefficients with least squares criterion and differing by the control of the degree of smoothness of the fitted curves. P-splines add a penalty term in the least square's equation so that the lack of smoothness in the curves is controlled by a smoothing parameter λ [39]. Obviously, the degree of smoothness in the fitted curves influences the statistical analysis and the data interpretation. Therefore, the researcher, according to the goal of the experiment and the nature of the measure should define such adjustment. Fig. 4 shows two different approximations by using regression splines, defined on 17 not equally spaced nodes (at the top) and P-splines defined on 17 equally spaced nodes with $\lambda = 0.11$ (at the bottom). For each approximation, the fitted curves for a normoglycemic (left panel) and a hyperglycemic (right panel) cases are shown in Fig. 4. Both approximations will be discussed in the results section.

B. Functional Principal Component Analysis

A functional principal component analysis [40] was applied to the measured W-band data to explore and highlight variability among the estimated functional spectra, determining a set of uncorrelated functions called functional principal components (FPCs). The principal components are obtained as uncorrelated generalized linear combinations of the sample curves with maximum variance. In general, the *j*th principal component scores are given by

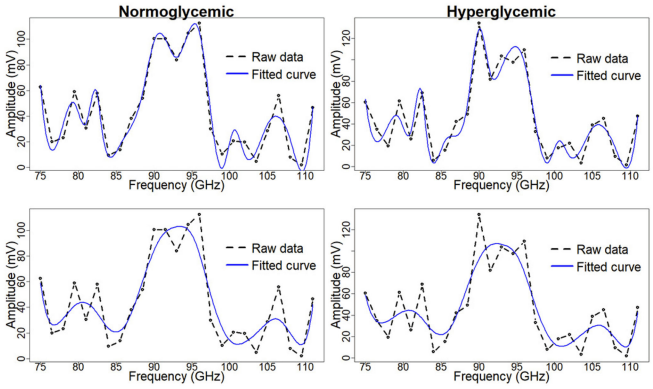

Fig. 4. Estimated and measured transmission amplitude for a normoglycemic (left panel) and a hyperglycemic mouse (right panel) by using two different approximations. Regression splines (at the top) defined on 17 not equally spaced nodes and P-splines (at the bottom) defined on 17 equally spaced nodes with $\lambda = 0.11$.

$$\xi_{ij} = \int_F x_i(f)\, w_j(f)\, df, \quad i = 1, \ldots, n \tag{3}$$

with w_j being the weight functions or loadings obtained by solving the following maximization problem, under the orthonormality constraints

$$\begin{cases} \max\limits_{w} \operatorname{var}\left[\int_F x_i(f)\, w(f)\, df\right] \\ \text{s.t.} \quad \|f\|^2 \text{ and } \int_T w_j(f)\, w_l(f)\, df = 0 \quad \forall j < l \end{cases}. \tag{4}$$

For more details, see [32]. The advantages of working with FPCs are the reduced dimensionality of the statistical problem and avoidance of multicollinearity problems in the regression analysis.

C. Functional Principal Component Logit Regression

The detection of sustained hyperglycemia has been addressed as a classification problem with a binary response: normoglycemia or hyperglycemia. Therefore, we applied functional logit regression [41] to obtain a predictive model. The logit regression is widely used in social and medical applications, modeling qualitative variables by a set of independent variables as predictors. The functional logit model (FLoR) is the extension of the logit regression to the FDA context, but in this case, the predictor is a functional variable. The FLoR model is formulated as follows:

$$y_i = \pi_i + \epsilon_i, \quad i = 1, \ldots, n \tag{5}$$

where $y_i \in \{0, 1\}, \quad i = 1, \ldots, n$ is the value of the response variable associated with the *i*th observation of the functional predictor $x_i(f)$, being $0 \equiv$ normoglycemia and $1 \equiv$ hyperglycemia, ϵ_i are the independent errors with zero mean and

$\pi_i = P[Y = 1|\{x_i(f) : f \in F\}]$ is the expectation of the response variable given by

$$\pi_i = \frac{\exp\left\{\alpha + \int_F x_i(f)\,\beta(f)\,df\right\}}{1 + \exp\left\{\alpha + \int_F x_i(f)\,\beta(f)\,df\right\}}, \quad i = 1, \ldots, n. \quad (6)$$

As it can be seen in (6), π_i is modeled by a real parameter α and a functional parameter $\beta(f)$. Equivalently, (6) can be rewritten in terms of the logit transformation as follows:

$$l_i = \ln\left[\frac{\pi_i}{1-\pi_i}\right] = \alpha + \int_F x_i(f)\,\beta(f)\,df, \quad i = 1, \ldots, n. \quad (7)$$

In order to solve the estimation problems in the FLoR model, a set of FPCs can be used as predictor variables [35]. Then, the FLoR model can be expressed in matrix form in terms of a reduced set of *q* principal components (FPCLoR) as follows:

$$L = \alpha + \Gamma\gamma \quad (8)$$

with $\Gamma = (\xi_{ij})_{nxq}$ being the matrix comprising the columns of the first q principal components and γ being the vector of the model coefficients. Finally, by assuming the basis representation of the functional parameter $\beta(f)$ and the weight functions $w_j(f), \quad j = 1, \ldots, p$, the functional parameter of the FLoR model is estimated by $\beta = \mathbf{M}_{(pxq)}\gamma_{(qx1)}$, where $\beta = (\beta_1, \ldots, \beta_p)'$ is the vector of basis coefficients of $\beta(f)$ and $\mathbf{M}$ is a matrix whose columns contain the vectors of basis coefficients of the weight functions associated with the first q principal components [35].

A significant additional contribution of the FLoR is the interpretation of $\beta(f)$. This function represents the relation between the response variable and the functional predictor, and it can be interpreted in terms of the odds ratio [42]. Let us consider l_i the logit transformation of a sample function $x_i(f)$ and l_i^* is a resulting scaled logit transformation of a sample function $x_i^*(f)$ scaled by the factor K within a frequency bandwidth $[f_0, f_{0+h}] \subseteq F$. Then, the odds ratio for l_i and l_i^*, considering (7) will be

$$\exp(l_i^* - l_i) = \exp\left(K \int_{f_0}^{f_{0+h}} \beta(f)\,df\right). \quad (9)$$

This means that a constant increment in *K* units in a fixed interval for $x(f)$ increases the odds of $y = 1$ against $y = 0$ by a factor of the same magnitude *K*. This kind of interpretation is very useful to understand the relation between the spectral response, measured by the spectroscopic system and the achieved classification. This interpretation provides not only information (in the quantitative sense) about the aimed discrimination but also it can be useful to identify which interrogation frequency intervals are more relevant for such discrimination. This approach will be illustrated in the results section by interpreting the FPCLoR for the sustained hyperglycemia detection in animal models.

IV. Results and Discussion

This section focuses on the robustness and prediction of the diagnostic tool utilizing W-band measured spectra. First, sample B is used for a multitest analysis to study the performance and robustness of the fitted model for hyperglycemia discrimination. In this article, the results obtained from both approximations, regression splines and P-splines, will be compared. Then, in subsection IV-B, the diagnostic tool will be validated by testing the prediction capability of the fitted model on the sample A. Additionally, the FPCLoR model is analyzed by interpreting the functional parameter. All the data processing and analysis were performed using the statistical software R project [43], and the *fda* package [44].

TABLE II
Confusion Matrix

		True condition	
		Hyperglycemia	**Normoglycemia**
Predicted condition	**Hyperglycemia**	Hyperglycemia correctly classified (True Positive)	Normoglycemia misclassified (False Positive)
	Normoglycemia	Hyperglycemia misclassified (False Negative)	Normoglycemia correctly classified (True Negative)

An important observation of the diagnostic tool is that the measured amplitude of the transmitted skinfold signals is sufficient for accurate analysis. Even though the phase of the signal is also acquired by the spectroscopy system, results did not improve when taking phase into account. Furthermore, there is no need to preprocess or calibrate the amplitude data.

A. Multitest Analysis: Performance and Robustness of the Diagnostic Tool

The functional data obtained from sample B was employed for a multitest analysis. As reported in Table I, the functional data contains 33 observations. The training sample consisted of 80% of the functional data and the remaining 20% were assigned as a test sample. The observations for each group were selected randomly by preserving the original proportion of both classes within the global group: 54% of the cases are normoglycemic and 46% are hyperglycemic. Then, an FPCLoR model was fitted from the training sample, and the test sample was used to assess the prediction of the model. This process was repeated 100 times, and every time the performance of the predictive model was evaluated measuring four validation parameters: the area under ROC curve (AUC), true positive rate (TPR), true negative rate (TNR), and correct classification rate (CCR). The TPR and TNR, also known as sensitivity and specificity, respectively, are commonly used in medical diagnostics [45]. The TPR, TNR, and CCR values are estimated taking into account the confusion matrix, listed in Table II, as follows:

$$\mathrm{TPR} = \frac{\mathrm{TP}}{\mathrm{TP} + \mathrm{FN}}, \quad \mathrm{TNR} = \frac{\mathrm{TN}}{\mathrm{TN} + \mathrm{FP}},$$
$$\mathrm{CCR} = \frac{\mathrm{TP} + \mathrm{TN}}{\mathrm{TP} + \mathrm{TN} + \mathrm{FP} + \mathrm{FN}}.$$

The receiver operating characteristic (ROC) curve shows the inverse relationship between the sensitivity and the specificity (sensitivity versus 1-specificity) varying the diagnostic criterion (the defined value to assign $y = 1$) of the test, and the AUC, which can be estimated by numerical integration methods,

TABLE III
SUMMARY OF THE MULTITEST ANALYSIS

Parameter	Regression splines		P-splines	
	Mean	Std. Dev.	Mean	Std. Dev.
AUC	0.99	0.01	0.96	0.02
CCR	0.92	0.08	0.82	0.11
TPR	0.91	0.18	0.74	0.23
TNR	0.93	0.11	0.87	0.18

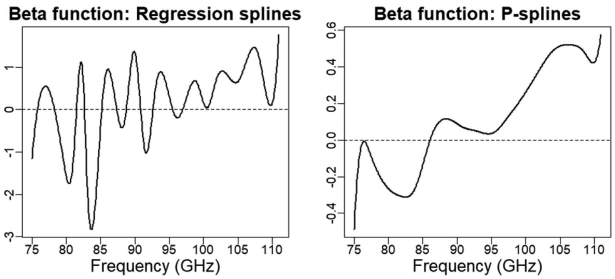

Fig. 5. Functional parameter $\beta(t)$ estimated for FPCLoR on the functional data approximated by regression splines and P-splines (left and the right, respectively).

provides an effective measure of the diagnostic accuracy of the predictive model. Table III summarizes the results of the multitest analysis for both approximations: regression splines and P-splines (see Fig. 4).

Comparing both cases, we can see that the mean value of AUC is slightly higher for the model based on regression splines than P-splines. However, for both cases, this value is above 0.95 (excellent discrimination capability) and very robust with a standard deviation under 0.02. This indicates that the FPCLoR model clearly discriminates the intercondition (normoglycemia and hyperglycemia) variability captured by the spectroscopic instrument. As listed in Table III, the predictive capabilities for both cases are very good with a mean value of CCR above 80%, being 10% higher for the case of regression splines. These results suggest that the FPCLoR model obtained from regression splines is the best in terms of the prediction capabilities. Nevertheless, as mentioned above, a significant advantage of working with the FPCLoR is the interpretation of the estimated functional parameter $\beta(f)$, which offers relevant information to improve the diagnostic tool. Here, we can emphasize that the lack of smoothness in the functional data is reflected in the estimated functional parameter. Fig. 5 shows one of the functional parameters estimated for both approaches, based on regression splines (left panel) and P-splines (right panel). The functional parameter estimated from the regression splines exhibits strong oscillation versus frequency making its interpretation difficult. Considering a noisy function, as obtained from the regression splines, it can be seen in (9) that the frequency domain must be divided into several subintervals so that the integral of the beta function does not tend to zero, which implies an estimated odds ratio close to one. This minimizes the contribution of the frequencies for discrimination and forces to consider very short frequency intervals, losing a lot of information. On the other hand, a smoother functional parameter is obtained by the P-spline approach. Therefore, in the

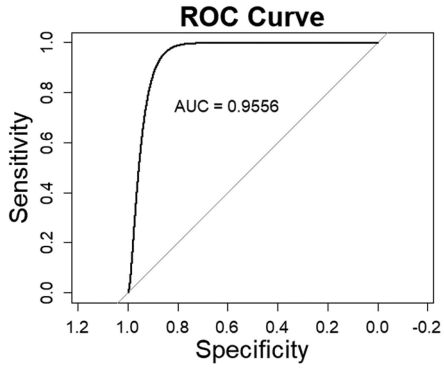

Fig. 6. ROC curve estimated for the FPCLoR model.

Section IV-B, we will work with the P-splines since the resulting functional parameter offers much better interpretation of the FPCLoR model and both provide excellent multitest results.

B. Validation and Analysis of the Diagnostic Tool

The multitest analysis showed that the diagnostic tool allows for correct diagnosis (detection) of hyperglycemia in animal models with excellent and very robust results. Then, sample A, measured at a second experiment, was used to validate the consistency of the diagnostic tool to discriminate the condition in a new sample. Once again, an FPCLoR model was fitted using the 33 mice from sample B as a training sample, and sample A was the test sample. As reported in Table I, sample A consists of 20 mice with hyperglycemia and normoglycemia proportionately distributed. Functional data from both sample A and sample B were estimated by using P-splines defined on 17 equally spaced points in the spectrum, as shown in Fig. 4 (bottom). The ROC curve corresponding to the fitted model is shown in Fig. 6 with the AUC $= 0.95$. Testing the prediction capabilities of the fitted FPCLoR model on the test sample, we obtain a 100% on the new observations correctly classified (CCR). These results validate the consistency of the measured spectral response for sustained hyperglycemia, and consequently, support the reliability of the spectroscopy instrument.

Finally, the functional parameter for the sustained hyperglycemia discrimination obtained from the FPCLoR model is shown in Fig. 7. As a first observation, we notice that the beta function varies from negative to positive values versus frequency with a zero crossing at 86 GHz, indicated by a red line. The frequency interval is then subdivided into two sections, which inversely relate the spectral response and the hyperglycemia. To illustrate this, we will interpret the odds ratio for both frequency intervals considering a constant increase in the measured transmission amplitude of 0.3 mV $(K = 0.3)$ for the spectral response. The estimated odds ratio for both frequency intervals is presented in (10) and indicates that such a constant increment in the transmitted amplitude for frequencies under 86 GHz reduces the odds of being diabetic to one half, in contrast to frequencies above 86 GHz, where the odds is sixfold. In this way, we are able to measure the impact of a change in the spectral response in the diagnosis, enabling further development of a quantified diagnostic measure for accurate diagnosis in the management

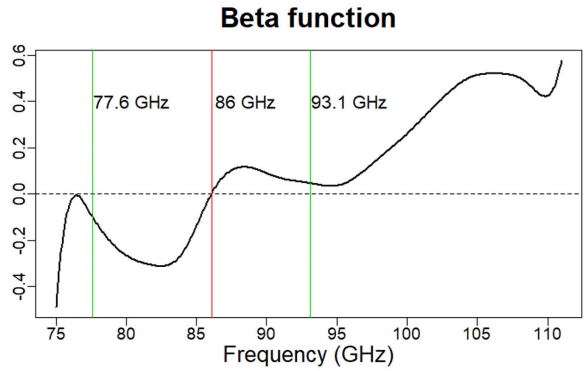

Fig. 7. Discriminating function $\beta(t)$ for sustained hyperglycemia detection of the FPCLoR model. The red line indicates a sign change for the function at the frequency of 86 GHz. The green lines indicate the frequencies, chosen arbitrarily, as the lower and upper limits for a reduced frequency band.

of diabetes

$$\mathrm{OR}_{75-86}^{0.3} = 0.516 \; OR_{86-111}^{0.3} = 6.52\,. \tag{10}$$

Additionally, to show the potential of the statistical approach, we reduce the frequency band, keeping the inflection point of the functional parameter ($\sim$86 GHz) within the band, with the lower and upper frequency limit chosen arbitrarily to be 78 GHz and 93 GHz, respectively, indicated by green lines in Fig. 7. The frequency range was delimited around the frequency in which the functional parameter crosses zero since that frequency interval provides two regions which relate strongly and inversely the spectral response to the hyperglycemia condition, enhancing the discrimination. The reduction of the frequency range represents a drastic improvement in measurement time if one can assume to use the same frequency step. It also has an important impact of instrument complexity. However, since less frequencies are considered, less information is provided to the regression model that may affect the discrimination. Therefore, the discrimination of sustained hyperglycemia was evaluated on the new measurement span (78–93 GHz). As before, an FPCLoR model was fitted for the resulting set of functional data estimated from the reduced spectra corresponding to sample B. Then, the prediction capability of the FPCLoR model was tested on sample A. For both datasets, functional data were approximated by P-splines defined on 11 equally spaced spectral points with $\lambda = 0.528$. The validation parameters of the fitted FPCLoR model for the selected frequency interval are AUC $= 1$, CCR $= 0.95$, TPR $= 0.90$, and TNR $= 1$. This represents an improvement in discrimination as compared to Table III. This improvement is attributed to the fact that the major contribution to the discrimination in our case originates from this frequency interval and the remaining frequency interval is essentially contributing to potential errors to the overall analysis.

V. Conclusion

This article demonstrates the suitability of mm-wave spectroscopy in the W-band for hyperglycemia discrimination using advanced statistical methods. The article also shows that the model developed here is predictive and provides excellent results across several independent tests. The results obtained for sustained hyperglycemia discrimination and prediction, which are strongly related to diabetes condition, were based on the spectral data from the transmission reflection setup covering the full W-band.

The spectral data employed in this article are based on the transmission amplitude data only, demonstrating that the amplitude spectrum contains the major information, leading to the conclusion that transmission through the skinfold is important. An advantage of this technique is its inherent insensitivity to skin reflectivity. Moreover, no previous calibration by a reference response from the spectrometer has to be performed to the measured amplitude prior to the statistical analysis. These results simplify the overall spectroscopy system resulting in a simple transmission-type spectrometer with a limited frequency bandwidth of operation. We also show that interpreting the FPCLoR model allows us to detect the most contributing frequencies for discrimination so that the spectral interrogation can be optimized by selecting a substantially narrower frequency band enough for discrimination.

A major contribution lies in the advanced statistical techniques (functional data analysis) applied to the mm-wave spectroscopy data. We have used a set of measured spectra representative of different glycemic states in animal models. Normoglycemic mice with an expected blood glucose level $\sim$100 mg/dL and mice suffering sustained hyperglycemia with chronically elevated levels of glucose in blood $>$150 mg/dL were noninvasively tested by the mm-wave instrument. The transmitted amplitude data were evaluated by applying FPCLoR, thus obtaining a predictive model for sustained hyperglycemia, typically associated with diabetes. The analysis was carried out by combining a nonspecific approach and FDA. A multitest analysis, with 100 iterations, was performed on a sample of 33 mice (18 normoglycemic cases and 15 hyperglycemic cases) studying two different approaches for the approximation of the functional data: regression splines and P-splines. The mean values for both approaches in an AUC > 0.95 and in a CCR $> 80\%$. The multitest analysis shows that the discrimination of hyperglycemia was slightly better-using regression splines, but the lack of smoothness in the approximation of the functional data makes it difficult to interpret the fitted model. Considering the roughness of the approximation for functional data, we were able to reduce the spectral frequency range by almost one half, with only a 5% penalty, as the CCR decreased from 100% to 95% in the validated predictive model. These results indicate the great applicability of combining the mm-wave spectroscopy with a nonspecific approach for new noninvasive diagnostic tools, and the potential of the FDA developing spectroscopic diagnostic tools.

References

[1] G. G. Hernandez-Cardoso *et al.*, "Terahertz imaging for early screening of diabetic foot syndrome: A proof of concept," *Sci. Rep.*, vol. 7, 2017, Art. no. 42124.

[2] J. Y. Sim, C.-G. Ahn, E.-J. Jeong, and B. K. Kim, "In vivo microscopic photoacoustic spectroscopy for non-invasive glucose monitoring invulnerable to skin secretion products," *Sci. Rep.*, vol. 8, 2018, Art. no. 1059.

[3] Y. Nikawa and T. Michiyama, "Non-invasive measurement of blood-sugar level by reflection of millimeter-waves," in *Proc. Asia-Pac. Microw. Conf.*, 2006, pp. 47–50.
[4] P. H. Siegel *et al.*, "Compact non-invasive millimeter-wave glucose sensor," in *Proc. 40th Int. Conf. Infrared, Millimeter, Terahertz Waves*, 2015, pp. 1–3.
[5] B. M. Garin, V. V. Meriakri, E. E. Chigrai, M. P. Parkhomenko, and M. G. Akat'eva, "Dielectric properties of water solutions with small content of glucose in the millimeter-wave band and the determination of glucose in blood," *PIERS Online*, vol. 7, pp. 555–558, 2011.
[6] P. H. Siegel, Y. Lee, and V. Pikov, "Millimeter-wave non-invasive monitoring of glucose in anesthetized rats," in *Proc. 39th Int. Conf. Infrared, Millimeter, Terahertz Waves*, 2014, pp. 1–2.
[7] S. F. Clarke and J. R. Foster, "A history of blood glucose meters and their role in self-monitoring of diabetes mellitus," *Brit. J. Biomed. Sci.*, vol. 69, no. 2, pp. 83–93, Aug. 2012.
[8] W.-C. Shih, K. L. Bechtel, and M. V. Rebec, "Noninvasive glucose sensing by transcutaneous Raman spectroscopy," *J. Biomed. Opt.*, vol. 20, no. 5, May 2015, Art. no. 051036.
[9] S. Liakat *et al.*, "Noninvasive in vivo glucose sensing on human subjects using mid-infrared light," *Biomed. Opt. Express*, vol. 5, no. 7, pp. 2397–2404, Jul. 2014.
[10] E. Ryckeboer, R. Bockstaele, M. Vanslembrouck, and R. Baets, "Glucose sensing by waveguide-based absorption spectroscopy on a silicon chip," *Biomed. Opt. Express*, vol. 5, no. 5, pp. 1636–1648, May 2014.
[11] P. Martín-Mateos *et al.*, "In-vivo, non-invasive detection of hyperglycemic states in animal models using mm-wave spectroscopy," *Sci. Rep.*, vol. 6, 2016, Art. no. 34035.
[12] C. D. Mathers and D. Loncar, "Projections of global mortality and burden of disease from 2002 to 2030," *PLoS Med.*, vol. 3, no. 11, 2006, Art. no. e442.
[13] M. Danny, P. McGovern, and R. Safadi, "An epidemiological overview of diabetes across the world," *Brit. J. Nursing*, vol. 16, no. 16, pp. 1002–1007, Sep. 2007.
[14] K. Ogurtsova *et al.*, "IDF diabetes atlas: Global estimates for the prevalence of diabetes for 2015 and 2040," *Diabetes Res. Clin. Pract.*, vol. 128, pp. 40–50, 2017.
[15] J. R. Bain *et al.*, "Metabolomics applied to diabetes research: Moving from information to knowledge," *Diabetes*, vol. 58, no. 11, pp. 2429–2443, Nov. 2009.
[16] N. Friedrich, "Metabolomics in diabetes research," *J. Endocrinol.*, vol. 215, no. 1, pp. 29–42, Oct. 2012.
[17] Expert Committee on the Diagnosis and Classification of Diabetes Mellitus, "Report of the expert committee on the diagnosis and classification of diabetes mellitus," *Diabetes Care*, vol. 26, no. Suppl 1, pp. S5–20, Jan. 2003.
[18] K. G. M. M. Alberti and P. Z. Zimmet, "Definition, diagnosis and classification of diabetes mellitus and its complications. Part 1: Diagnosis and classification of diabetes mellitus provisional report of a WHO consultation," *Diabetes Med.*, vol. 15, no. 7, pp. 539–553, 1998.
[19] D. M. Nathan, "Long-term complications of diabetes mellitus," *New England J. Med.*, vol. 328, no. 23, pp. 1676–1685, Jun. 1993.
[20] J. Yadav, A. Rani, V. Singh, and B. M. Murari, "Prospects and limitations of non-invasive blood glucose monitoring using near-infrared spectroscopy," *Biomed. Signal Process. Control*, vol. 18, pp. 214–227, 2015.
[21] D. Rodbard, "Continuous glucose monitoring: A review of successes, challenges, and opportunities," *Diabetes Technol. Ther.*, vol. 18, no. S2, pp. S3–S13, 2016.
[22] A. Nawaz, P. Øhlckers, S. Sælid, M. Jacobsen, and M. N. Akram, "Review: Non-invasive continuous blood glucose measurement techniques," *J. Bioinform. Diabetes*, vol. 1, no. 3, pp. 1–27, 2016.
[23] S. K. Vashist, "Non-invasive glucose monitoring technology in diabetes management: A review," *Analytica Chimica Acta*, vol. 750, pp. 16–27, Oct. 2012.
[24] T. Lin, A. Gal, Y. Mayzel, K. Horman, and K. Bahartan, "Non-invasive glucose monitoring: A review of challenges and recent advances," *Current Trends Biomed. Eng. Biosci.*, vol. 6, no. 5, pp. 1–8, 2017.
[25] J. C. L. Alves, C. B. Henriques, and R. J. Poppi, "Determination of diesel quality parameters using support vector regression and near infrared spectroscopy for an in-line blending optimizer system," *Fuel*, vol. 97, pp. 710–717, 2012.
[26] R. M. Balabin, R. Z. Safieva, and E. I. Lomakina, "Gasoline classification using near infrared (NIR) spectroscopy data: Comparison of multivariate techniques," *Analytica Chimica Acta*, vol. 671, no. 1/2, pp. 27–35, 2010.
[27] C.-W. Chang, D. A. Laird, M. J. Mausbach, and C. R. Hurburgh, "Near-infrared reflectance spectroscopy–principal components regression analyses of soil properties," *Soil Sci. Soc. Amer. J.*, vol. 65, no. 2, pp. 480–490, 2001.
[28] F. J. Wyzgoski *et al.*, "Modeling relationships among active components in black raspberry (Rubus occidentalis L.) fruit extracts using high-resolution (1)H nuclear magnetic resonance (NMR) spectroscopy and multivariate statistical analysis," *J. Agricultural Food Chem.*, vol. 58, no. 6, pp. 3407–3414, 2010.
[29] S. Hahn and G. Yoon, "Identification of pure component spectra by independent component analysis in glucose prediction based on mid-infrared spectroscopy," *Appl. Opt.*, vol. 45, no. 32, pp. 8374–8380, 2006.
[30] E. Andries and S. Martin, "Sparse methods in spectroscopy: An introduction, overview, and perspective," *Appl. Spectrosc.*, vol. 67, no. 6, pp. 579–589, 2013.
[31] F. Liu, Y. He, and L. Wang, "Determination of effective wavelengths for discrimination of fruit vinegars using near infrared spectroscopy and multivariate analysis," *Analytica Chimica Acta*, vol. 615, no. 1, pp. 10–17, 2008.
[32] J. O. Ramsay and B. W. Silverman, *Functional Data Analysis*. New York, NY, USA: Springer, 2013.
[33] H. Sørensen, J. Goldsmith, and L. M. Sangalli, "An introduction with medical applications to functional data analysis," *Statist. Med.*, vol. 32, no. 30, pp. 5222–5240, 2013.
[34] Z. Barati, I. Zakeri, and K. Pourrezaei, "Functional data analysis view of functional near infrared spectroscopy data," *J. Biomed. Opt.*, vol. 18, no. 11, 2013, Art. no. 117007.
[35] M. Escabias, A. M. Aguilera, and M. J. Valderrama, "Principal component estimation of functional logistic regression: Discussion of two different approaches," *J. Nonparametric Statist.*, vol. 16, no. 3/4, pp. 365–384, Jul. 2004.
[36] F. Dornuf *et al.*, "Classification of skin phenotypes caused by diabetes mellitus using complex scattering parameters in the millimeter-wave frequency range," *Sci. Rep.*, vol. 7, 2017, Art. no. 5822.
[37] T. A. Lutz and S. C. Woods, "Overview of animal models of obesity," *Current Protocols Pharmacol.*, vol. 58, no. 1, pp. 5.61.1–5.61.18, 2012.
[38] C. De Boor, *A Practical Guide to Splines*. New York, NY, USA: Springer, 2001.
[39] P. H. C. Eilers and B. D. Marx, "Flexible smoothing with B-splines and penalties," *Statist. Sci.*, vol. 11, no. 2, pp. 89–102, 1996.
[40] J. C. Deville, "Méthodes statistiques et numériques de l'analyse harmonique," *Annales L'insee.*, no. 15, pp. 3–101, 1974. [Online]. Available: https://www.jstor.org/stable/20075177?seq=1#metadata_info_tab_contents. Accessed on Feb. 12, 2020.
[41] G. M. James, "Generalized linear models with functional predictors," *J. Roy. Statist. Soc.*, vol. 64, no. 3, pp. 411–432, 2002.
[42] M. Escabias, A. M. Aguilera, and M. J. Valderrama, "Modeling environmental data by functional principal component logistic regression," *Environmetrics*, vol. 16, no. 1, pp. 95–107, 2005.
[43] R Development Core Team, "R: A language and environment for statistical computing," 2008. [Online]. Available: https://www.r-project.org, [Accessed on: May 1, 2019].
[44] J. O. Ramsay, G. Hooker, and S. Graves, *Functional Data Analysis With R and MATLAB*. New York, NY, USA: Springer, 2009.
[45] K. Søreide, "Receiver-operating characteristic curve analysis in diagnostic, prognostic and predictive biomarker research," *J. Clin. Pathol.*, vol. 62, no. 1, pp. 1–5, 2009.

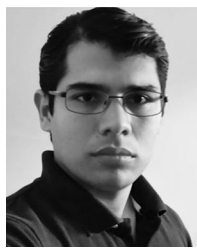

Aldo Moreno-Oyervides received the bachelor's degree in electronic engineering (honors) from the Instituto Tecnológico de Matamoros, Matamoros, México, in 2011 and the master's degree in mathematical engineering (with a competitive grant) in 2016 from the Universidad Carlos III de Madrid, Madrid, Spain, where he is currently working toward the Ph.D. degree with the Department of Electronic Technology with a grant by Consejo Nacional de Ciencia y Tecnología de México.

His research interests include the development of applied spectroscopy systems for complex structures by applying advanced statistical techniques.

M. Carmen Aguilera-Morillo received the degree in statistics (with honors) from the Universidad de Jaén, Jaén, Spain, in 2006, and the bachelor's degree in science and statistical techniques (honors), the master's degree in applied statistics, and the Ph.D. degree in statistics from the Universidad de Granada, Grande, Spain, in 2008, 2009, and 2013, respectively.

She received a Postdoctoral grant and was later hired as a Visiting Professor with the Universidad Carlos III de Madrid, Madrid, Spain, where she is currently a Juan de la Cierva Researcher with the Department of Statistics. Her research interests include penalized estimation methods for functional data analysis and its application to hematologic malignancies, spectroscopy, and the development of algorithms for variable selection in high-dimensional data and their application to real problems, such as breast cancer.

Dr. Aguilera-Morillo has been the Coordinator of the national working group on functional data analysis until 2017 (working group endorsed by the Spanish Society of Statistics and O. R. - SEIO). Her academic and professional trajectory has been recognized with eight awards: two extraordinary awards; first national prize; two prizes for the best record in Andalusia awarded by the Statistics Institute of Andalusia; prize from the Academy of Social Sciences and Environment of Andalusia and Unicaja; Ramiro Melendreras Prize, awarded by the Spanish Society of Statistics and O. R.; Health Innovation Prize 2017 (Hematology area), and awarded by the Celgene Chair of Universidad de Alcalá (in collaboration with researchers from the Gregorio Marañón Hospital).

Fernando Larcher received the B.S. and Ph.D. degrees in biochemistry from the School of Pharmacy and Biochemistry of the University of Buenos Aires, in 1984 and 1990, respectively.

His postdoctoral career took place with CIEMAT, Madrid, Spain, under the supervision of Dr. J. Jorcano working also on mouse skin carcinogenesis in several transgenic mouse models including those modulating EGFR signaling and angiogenesis. After short stays with the Living skin bank in Stony Brook, NY, USA, (PI, Dr. M. Simon) and with the DFKZ, Heidelberg (PI, Dr. P. Boukamp), in 1994 and 1995, respectively. He started studies using human keratinocytes with the purpose of developing cell and gene therapy approaches for skin diseases. He focused his studies first on the possibility of using genetically modified skin as a bioreactor. Later on, he became an independent Researcher focusing efforts in skin regenerative medicine aiming with the generation of several skin humanized animal models of rare skin diseases and novel approaches (advanced therapies) to correct their genetic defects. The development of these models was possible thanks to innovative cutaneous bioengineering approaches. Nowadays, in collaboration with Dr. M. D. Rio (joint unit UC3M-CIEMAT) and as a part of the Spanish Research Network for Rare Diseases (CIBERER), his laboratory is devoted to the translational research in rare skin disorders covering various aspects that include basic research and gene therapy protocols at preclinical and clinical stages. He is the author of 95 PubMed indexed scientific publications with an h factor of 32.

Viktor Krozer (Senior Member, IEEE) received the Dipl. Ing. and Dr. Ing. degrees in electrical engineering from Technical University (TU) Darmstadt, Darmstadt, Germany, in 1984 and in 1991, respectively.

In 1991, he became a Senior Scientist with TU Darmstadt working on high-temperature microwave devices and circuits and submillimeter-wave electronics. From 1996 to 2002, he was a Professor with the Technical University of Chemnitz, Chemnitz, Germany. During 2002–2009, he was a Professor with Electromagnetic Systems, DTU Elektro, Technical University of Denmark, and was heading the Microwave Technology Group. During 2009–2012, he was an endowed Oerlikon-Leibniz-Goethe Professor for Terahertz Photonics with Johann Wolfgang Goethe University Frankfurt, Germany, where he has been heading the Goethe-Leibniz-Terahertz-Center since 2012. He is also with Ferdinand Braun Institut für Höchstfrequenztechnik, Berlin, Germany, leading the THz components and systems group. His research areas include terahertz electronics and imaging, MMIC, nonlinear circuit analysis and design, device modeling, biomedical sensors, and remote sensing instrumentation.

Pablo Acedo received the master's degree in telecommunication engineering from the Universidad Politécnica de Madrid, Madrid, Spain, in 1993, and the Doctorate (honors) from the Universidad Carlos III de Madrid, Madrid, Spain, in 2000 for his work on heterodyne two color laser interferometry for fusion plasma diagnostics.

His doctoral work has included the development of the first two color laser system based on Mid-IR sources for a Stellarator Fusion Device (Stellarator TJ-II, Laboratorio Nacional de Fusión, CIEMAT, Madrid) and the first two-color Nd:YAG system for a Fusion Device (Tokamak C-Mod Plasma Science and Fusion Centre, Massachusetts Institute of Technology), the later during several doctoral visits to MIT during the years 1996–1999. In 2002, he was appointed as a Assistant Professor by the Universidad Carlos III de Madrid, where he continued with the development of scientific instrumentation systems for fusion plasma diagnostics and biomedical applications, leading national projects and contracts on these fields. Starting 2009, his research interests focused on the development of multimode laser sources (optical frequency combs) and their applications in photonic signal synthesis with the development of several architectures for the generation, detection, and processing of THz signals, leading several research projects and contracts in this field. In 2014, he demonstrated with his team one of the first implementations of dual-optical frequency comb architectures based on electrooptical modulators and its use in dispersion spectroscopy, and other applications beyond spectroscopy, which has made him an international reference in this type of optical sources. In 2013, he intensified his activity in biomedical applications including the development of diagnostics, such as an instrument for the early detection of vascularization in engraftments with applications in tissue engineering, and a noninvasive system for the measurement of sustained states of hyperglycemia. He has authored or coauthored more than 130 articles in high-impact journals and communications to International Congresses, including invited conferences and seminars. He has also directed nine research projects (European, national, and regional funding) and has participated in another 31 (five of them EU funded). Finally, it is worth mentioning his leadership in knowledge transfer activities, where he has been IP in 12 contracts with companies (INDRA, AIRBUS D&S, LWL, SEAC, …) and participated in another six; works that have led to various patents. He was also the promoter of the creation and development of the spin-off Luz Wave-Labs (www.luzwavelabs.com), which exploits most of his developments in the photonic synthesis of THz and pulsed optical sources. Nowadays, his interests continue to focus on the development of scientific instrumentation systems, sensors and circuits, and their application in fields, such as bioengineering and environmental measurements.